

International Conference PLASMA-2013, Warsaw, Sept. 2 – 6, 2013

P - 1.14

## ATOMIC DATA AND COLLISIONAL-RADIATIVE MODEL FOR BERYLLIUM AND ITS IONS

D. Kondratyev<sup>1\*</sup>, O. Marchuk<sup>1</sup>, L. Vainshtein<sup>2</sup>, I. Bray<sup>3</sup>, D. Fursa<sup>3</sup>, Y. Ralchenko<sup>4</sup>, D. Reiter<sup>1</sup>

<sup>1</sup>*Forschungszentrum Jülich GmbH, Institute of Energy and Climate Research - Plasma Physics,  
EURATOM Association, 52425 Jülich, Germany*

<sup>2</sup>*P.N.Lebedev Physical Institute RAS, Leninsky prospect 53, Moscow, 119991 Russia*

<sup>3</sup>*ARC Centre of Excellence for Antimatter-Matter Studies, Curtin University, Perth, Western Australia, Australia*

<sup>4</sup>*National Institute of Standards and Technology, Gaithersburg, Maryland 20899, USA*

### Abstract

In this work we present a collisional-radiative model constructed for all ionization stages of beryllium. Convergent close-coupling, K-matrix and Coulomb-Born-exchange methods were applied to calculate the necessary atomic data. For neutral beryllium atom a comparison of all methods is given. Fractional ion abundances, radiative power losses and electron cooling rates were calculated as functions of electron temperature. The comparison with other available data shows a rather good agreement.

---

*PACS:* 52.20.Hv, 34.80.Dp

*PLASMA-2013 keywords:* Elementary processes, Beryllium, Collisional-radiative model

*\*Corresponding author address:* Forschungszentrum Jülich, IEK-4, 52425 Jülich, Germany

*\*Corresponding author E-mail:* [d.kondratyev@fz-juelich.de](mailto:d.kondratyev@fz-juelich.de)

*Presenting author:* Dr. Dmitry Kondratyev

*Presenting author E-mail:* [d.kondratyev@fz-juelich.de](mailto:d.kondratyev@fz-juelich.de)

# 1 Introduction

Beryllium is used in the ITER-like wall at JET and is foreseen as a plasma-facing material in the main chamber of ITER [1]. For interpretation of spectroscopic measurements and for modelling of the beryllium impurity behaviour in plasma, collisional atomic data (cross sections of elementary processes) are required. The “effective” rate coefficients given in existing atomic databases (e.g. ADAS [2]) are sometimes insufficient for applications. The formation of beryllium hydrides (BeH, BeH<sub>2</sub>) and their ions in the edge plasma and the subsequent fragmentation directly populating excited atomic states and affecting the measured light emission can be mentioned as an example. Unfortunately due to high toxicity of beryllium the experimental cross sections are practically unavailable in the literature. The most accurate theoretical methods, such as convergent close-coupling (CCC) [3] or the R-matrix with pseudostates (RMPS) [4] demand very large computation time (especially at intermediate energies when continuum coupling effects are important) and the corresponding cross sections (first of all, for transitions between excited states) are still fragmentary. For the overcoming the lack of data the relatively simple, fast and sufficiently accurate methods such as K-matrix [5] or Coulomb-Born with exchange and normalization can be applied.

In this paper, we present a collisional-radiative model (CRM) constructed for all ionization stages of beryllium. For neutral Be and selected transitions in Be<sup>+</sup> the sophisticated CCC method was used. The cross sections for ions Be<sup>2+</sup>, Be<sup>3+</sup> were computed by the code ATOM [6] using the K-matrix (for excitation) and the normalized Born (for ionization) methods. Also at the example of Beryllium atom we present a comparison between the K-matrix and CCC results. Supplementary data associated with this article (cross sections  $\sigma$ , rate coefficients  $\langle v\sigma \rangle$  as well as the adjusted parameters for fitting formulas) are partially presented on the website [7] and are available in electronic form upon request.

In the following, we use atomic units with the Rydberg unit for energy and temperature ( $Ry = 13.6$  eV). Cross sections are given in the units  $\pi a_0^2 = 0.8797 \cdot 10^{-16}$  cm<sup>2</sup> where  $a_0$  is the Bohr radius. We also use the designation:

$$[j_1 j_2 j_3 \dots] = (2j_1 + 1)^{1/2} (2j_2 + 1)^{1/2} (2j_3 + 1)^{1/2} \dots$$

## 2 Atomic data

### 2.1 K-matrix method

Here we confine ourselves to the consideration of transitions only between terms. The calculation of excitation cross sections based on the K-matrix method [5] was performed by the code ATOM-AKM [6] and consists of three parts.

1) A chosen list of atomic states (basis) is used as an input information. Usually the basis  $a = \gamma_c S_c L_c n l S L$  (where  $\gamma_c S_c L_c$  describe the atomic core,  $n l$  are the principal and orbital quantum numbers of the optical electron)

includes the ground state, all one-electron excitations with  $n$  from  $n_0$  up to  $n_{max}$  and maybe a few two-electron excitations.

2) For all pairs of states ( $a_i, a_f: E_i < E_f$ ) from the basis, for a set of partial waves ( $\lambda_i, \lambda_f$ ) of the outer electron and for total angular momenta  $S_T, L_T$  the transition amplitudes  $K^B$  (matrix elements of interaction) are calculated in  $B$  - approximation. Here and below we designate by the index  $B$  the Born (for neutral atoms) or Coulomb-Born (for ions) approximation with exchange between the incident and target electrons that we take into account using the orthogonalized wave-function method [8]. The mixing coefficients appearing in the configuration interaction expansion can be obtained from other sources (e.g. using the Cowan code [9]).

3) From transition amplitudes the full matrix  $\mathbf{K}^B$  is constructed. The final unitary scattering matrix  $\mathbf{S}$  is obtained according to the matrix equation [5]:

$$\mathbf{S} = \frac{\mathbf{I} + i\mathbf{K}^B}{\mathbf{I} - i\mathbf{K}^B} \quad (1)$$

where  $\mathbf{I}$  is the diagonal identity matrix. The cross sections are expressed in terms of  $\mathbf{S}$ -matrix [8]:

$$\sigma(a_i - a_f) = \frac{1}{2k_i^2} \sum_{\lambda_i \lambda_f L_T S_T} \frac{[S_T L_T]^2}{[S_i L_i]^2} |S_{\Gamma_i \Gamma_f} - \delta_{\Gamma_i \Gamma_f}|^2 \quad (2)$$

Here  $\Gamma = as\lambda S_T L_T$  is a full set of quantum numbers of the total system (“atom + incident electron”),  $S_T$  and  $L_T$  are the full spin and angular momenta and  $k_i^2$  is the energy of the incident electron before the collision.

We call such an approach the *K-matrix method*. This method permits to correct some important shortcomings of the  $B$ -approximations:

1) *Normalization*. The total flux of scattered electrons should not exceed the incident one. In any first-order method this requirement may be broken since the excitation amplitude  $K_{\Gamma_i \Gamma_f}^B$  is proportional to the interaction matrix element and not limited by any condition. The  $\mathbf{S}$ -matrix is unitary and the requirement of electron flux conservation (“normalization”) is automatically fulfilled. Normalization can considerably decrease the cross section of strong transitions, such as dipole or transitions between nearby levels  $nl_0 - nl_1$ . Equation (1) also includes the possibility of normalization of weak transitions for account of the strong transitions from the same initial level (normalization by another channel).

2) *Two-step transitions*. A direct quadrupole (for example,  $2s-3d$ ) transition cross section may be comparable (or smaller) than the two-step dipole one ( $2s-2p-3d$ ). This possibility is not included in  $\mathbf{K}^B$  but is provided by the transformation (1).

3) Other less straightforward consequences of the *channel interaction* are also reflected by the  $K$ -matrix method.

Note that the dimensions of matrix  $\mathbf{K}^B$  grow fast with the number of included states and partial waves. The sum over  $\lambda$  in equation (2) converges slowly. The numerical calculations include  $\lambda \leq \lambda_m$  (usually  $\lambda_m = 28$  was

used). The contribution  $\Delta\sigma(a_i - a_f)$  from  $\lambda > \lambda_m$  is calculated in the Born approximation.

The radial functions  $P_{nl}$  of atomic electron were obtained by numerical solution of the radial Schrödinger equation

$$\left[ \frac{d^2}{dr^2} - \frac{l(l+1)}{r^2} + 2\frac{\zeta_c(r/\omega)}{r} + \varepsilon(nlSL) \right] P_{nl}(r) = 0 \quad (3)$$

with the scaled potential  $U(r) = -\frac{1}{r}\zeta_c(r/\omega)$  where the effective atomic core charge  $\zeta_c(r)$  is calculated with the Slater functions. The energy parameter of the equation  $\varepsilon(nlSL)$  is equal to the experimental value of the level energy (from the ionization limit) and the scale parameter  $\omega$  is obtained as an equation eigenvalue. In most cases the NIST database [10] was used for  $\varepsilon(nlSL)$ .

## 2.2 Comparison of K-matrix and CCC cross sections

In order to investigate the accuracy of K-matrix method we compared the collision strengths and rate coefficients for neutral Be with results of more sophisticated CCC and RMPS calculations [11] (for RMPS only rate coefficients are published). The CCC cross sections are presented on the website [12] for transitions from the states with  $n = 2$  for collision energies  $E$  up to 1000 eV. Recently Igor Bray made more accurate calculations for all transitions with  $n \leq 4$ ,  $E \leq 400$  eV. The procedure was quite similar to the one described in [3] but included more target-space states (and pseudo-states): 293 in new and 108 in old calculations [3]. For energies below 10 eV (relative to the ground state) 10 partial waves were explicitly calculated, and 16 above. Extrapolation to infinity was done using the Born approximation.

The input data for K-matrix calculations included the following states:

$$2s^2 \ ^1S, 2snl \ ^1L, \ ^3L, L = l, n = 2 - 5, \text{ all } l,$$

$$2p^2 \ ^1S, \ ^3P, \ ^1D, \ 2p3l, l = 0 - 2$$

and the matrix CV of configuration interaction vectors. The states  $2p3l$  were used only for configuration mixing. The real transitions to these states were not considered. Corresponding levels are above the ionization threshold and their contribution to the channel interaction is negligible. The total number of transitions (including the elastic scattering channels) was equal to 393. The mixing coefficients of the matrix CV were adjusted to obtain the best coincidence of the oscillator strengths  $f$  with the results of MCHF calculations [13]. The mixing up to 4 configurations was included for every group of states with the same  $SL$  and parity.

For discussion of the results it is important to distinguish two energy ranges. At large energies collisional part of the problem is trivial: the cross section  $\sigma = \sigma^B$  where  $\sigma^B$  is the Born cross section (without exchange if  $\Delta S = 0$ ). The difference between K-matrix and CCC data is connected with the difference of the atomic wave functions, i.e. with the configuration mixing. At small and medium energies of the scattered electron the difference in the approach to the collisional part of the problem (i.e. the normalization and the channel interaction) is important. From the present results as well as our previous calculations we can conclude that the K-matrix method tends to overestimate the effect of the channel interaction. We divide (perhaps rather arbitrary) the cross sections into three

groups according to the degree of agreement with CCC:

1) *Good* agreement was obtained, as illustrated in figure 1a, for dipole transitions, if oscillator strength is not very small. We note also the significant influence of the configuration mixing. For intercombination transitions (fig. 1b) the difference is somewhat larger because the exchange is normally more sensitive to the used approximations. The too fast decrease of CCC cross section can be connected with insufficient number of partial waves to ensure convergence and the large peaks near threshold (resonances due to the virtual formation of the  $\text{Be}^-$  ion) - with overestimation of exchange due to nonorthogonality of total wave functions (“residual Born-Oppenheimer”).

2) *Poor* agreement was found in cases of very strong configuration interaction when the description of atomic structure used in ATOM can be inadequate and for transitions with extremely small values of oscillator strengths for which the cancellation effects are important (fig. 1c).

3) Some *problematic* cases for which we cannot give a definite explanation. One example is shown in fig. 1d. For this transition ( $2s^2 \ ^1S \rightarrow 2p^2 \ ^1D$ ) two mechanisms are possible: the “step”  $2s^2 \ ^1S \rightarrow 2s2p \ ^1P \rightarrow 2p^2 \ ^1D$  (with asymptotic  $\Omega \sim \frac{1}{E}$ ) and the quadrupole transition ( $2p^2 \ ^1S \rightarrow 2p^2 \ ^1D$ ) due to configuration interaction  $2s^2 \ ^1S + 2p^2 \ ^1S$  (the asymptotic is  $\Omega \rightarrow \text{const}$ ). The collision strength of CCC, opposite to what we expect, increase. Maybe it can indicate the non-orthogonality of  $2p^2 \ ^1S$  and  $2p^2 \ ^1D$  states.

In most cases the agreement between rate coefficients is usually much better than for cross sections (even when there are substantial discrepancies for them). And of course the K-matrix results demonstrate essential improvement comparing to the Born data.

### 2.3 Electron impact ionization cross sections

For ionization of electron from the state  $a_i = \gamma_c S_c L_c n l_i S_i L_i$  of the atom (ion)  $X_z$

$$X_z(a_i) + e(E\lambda_i) \rightarrow X_{z+1}(\gamma_c S_c L_c) + e(E_f l_f) + e(E' \lambda_f), \quad E = E' + E_f + \Delta E \quad (4)$$

(here  $\Delta E = E_z$  is the ionization threshold) the ionization cross section in the *B*-approximation is equal:

$$\sigma_{iz}(nl_i) = \sum_{l_f S_f L_f} \int_0^{E_m/2} 2\sigma(a_i, a_f) dE_f \quad (5)$$

where  $E_m = E - \Delta E$  and  $a_f = \gamma_c S_c L_c E_f l_f S_f L_f$ . In this case the final state of the atom belongs to the continuum, and therefore the continuum radial function  $P_f(r)$  must be used.

Due to additional sum over the momenta  $l_f, S_f, L_f$  and the integral over the energy  $E_f$  of the ejected electron the inclusion of ionization channel in the K-matrix scheme becomes unreasonable (and practically impossible, which is why we didn't include the ionization channels in the K-matrix for excitation). At the same time due to these summations the ionization cross section  $\sigma_{iz}$  is not sensitive to the *channels interaction*. However the *normalization* effects must be included in the calculation of  $\sigma_{iz}$ .

The code ATOM [6] calculates ionization cross sections in  $B$ -approximation with additional normalization for own (ionization channel) and some strong excitation channels (usually these are transitions to nearby levels which are dipole connected with the initial state). The method of normalization is also based on K-matrix, but with some simplifications appropriate for normalization purposes, namely, the approximate (reduced) K-matrix contained only those matrix elements which include the initial state  $\Gamma_i$ . It means that the normalization of each  $L_T S_T$  channel is performed independently.

The ion  $X_{z+1}$  can be produced either by direct ionization (DI) or through inner shell excitation of  $X_z$  followed by autoionization (EA). In our calculations both DI and EA processes were included. As a rule, DI dominates the total impact ionization cross section but the contribution of EA increases at energies above the corresponding threshold.

A comparison of the ionization cross section from the ground state of Be I obtained by  $B$  and CCC methods is shown in figure 2. The account for exchange by the orthogonalized function method [8] sometimes leads to the appearance of a noticeable (non-physical) peak in the cross section at near-threshold energies. For this reason we usually use  $B$ -data calculated with normalization but without exchange.

### 3 Collisional-radiative model

Collisional-radiative model constructed for all charge stages of beryllium contains 80  $LS$  - terms:

Be I:  $2s^2 \ ^1S$ ;  $2snl \ ^1L, \ ^3L, L = l, n = 2 - 4$ , all  $l$ ;  $2p^2 \ ^1D, \ ^3P$  (19 terms)

Be II:  $1s^2 nl \ ^2L, L = l, n = 2 - 6$ , all  $l$  (20 terms)

Be III:  $1s^2 \ ^1S$ ;  $1snl \ ^1L, \ ^3L, L = l, n = 2 - 4$ , all  $l$  (19 terms)

Be IV:  $nl \ ^2L, L = l, n = 1 - 6$ , all  $l$  (21 terms)

Be V (bare nucleus): (1 state)

and includes the following processes: spontaneous radiative decays, electron impact excitation and ionization, as well as radiative, dielectronic and three-body recombination. The plasma is supposed to be optically thin. The energies of levels and (if available) the oscillator strengths were taken from NIST database. A new improved set of CCC excitation and ionization cross sections for neutral beryllium as well as CCC data [14] for  $\text{Be}^+$  were used. For selected transitions in Be,  $\text{Be}^+$  and for ions  $\text{Be}^{2+}$ ,  $\text{Be}^{3+}$  the cross sections were computed by the code ATOM [6] (the K-matrix for excitation and the normalized Coulomb-Born-Exchange for ionization). Note that the method used in ATOM corresponds to perturbation theory with a small parameter  $1/Z$ , where  $Z$  is the spectroscopic symbol. Therefore, the method's accuracy is expected to be better for ions. The partial photorecombination rate coefficients for all ion stages were also calculated by the ATOM code. Three-body recombination rates were obtained from the principle of detailed balance. For dielectronic recombination (DR) rates the formula suggested in [15] was used. We also assumed that DR occurs from the ground state of the target ion into the highest state of the recombined ion. This assumption is reasonable for Be with rather small resonance transition energy.

The steady-state solution of the system of balance equations for ionization equilibrium and level populations

was obtained using the collisional-radiative code NOMAD [16]. As an illustration, figure 3 shows ionization balance and radiative power loss coefficient  $L_z = P_{rad}/N_e N_a$  as a function of electron temperature, for an assumed electron density  $N_e = 10^{13} \text{ cm}^{-3}$ . Here  $N_a = \sum_Z N^Z$  is the total beryllium density,  $P_{rad}$  is the radiated power ( $\text{W} \times \text{cm}^{-3}$ ) including line (due to the cascade transitions), recombination (radiative and dielectronic) as well as bremsstrahlung radiation:

$$P_l = \sum_{Zij} 1.6 \times 10^{-19} N_i^Z A_{ij}^Z \Delta E_{ij}^Z \quad (6)$$

$$P_{rec} = \sum_{Zij} 1.6 \times 10^{-19} \left( \alpha_{ji}^{rr} \left( I_{ij}^Z + \frac{3}{2} T_e \right) + \alpha_{ji}^{dr} \Delta \bar{E}_j^{Z+1} \right) N_e N_j^{Z+1} \quad (7)$$

$$P_{br} = 1.54 \times 10^{-32} \bar{g} N_e \sqrt{T_e} \sum_Z N^Z Z^2 \quad (8)$$

The summation in (6), (7) is made over all the transitions and all ions  $Z$ . In formula (8), the frequency-averaged free-free Gaunt factor  $\bar{g}$  has been taken equal to 1.2, and  $T_e$  is expressed in eV.

The two peaks in  $L_z$  - one at low and another one at high temperatures - correspond to Be/Be<sup>+</sup> and Be<sup>2+</sup>/Be<sup>3+</sup> (i.e.,  $L$  - and  $K$  - shell) radiation, respectively. The minimum at  $\simeq 10$  eV occurs due to the fact that the most abundant He-like ions Be<sup>2+</sup> cannot be excited at that temperature. Below 100 eV,  $L_z$  is dominated by bound-bound transitions. At higher temperatures beryllium becomes completely ionized and no longer produces the line radiation. The increase of density leads to a shift of the ionization equilibrium and, more important, to the competition of collisional deexcitation with radiative decays. As a result, the total power-loss coefficient at a given temperature decreases.

In an ionizing regime, which is of special interest for the modeling of light impurity transport, electron cooling rate  $\Lambda = P_e/N_e N_a$  (where  $P_e$  is the electron cooling power in  $\text{W} \times \text{cm}^{-3}$ ) is dominated by excitation and ionization:

$$P_{ex} = \sum_{Zij} 1.6 \times 10^{-19} N_e (\langle v \sigma_{ij} \rangle_{ex} N_i^Z - \langle v \sigma_{ji} \rangle_{dex} N_j^Z) \Delta E_{ij}^Z \quad (9)$$

$$P_{iz} = \sum_{Zij} 1.6 \times 10^{-19} N_e (\langle v \sigma_{ij} \rangle_{iz} N_i^Z - N_e \alpha_{ji}^{3bR} N_j^{Z+1}) \left( I_{ij}^Z + \frac{3}{2} T_e \right) \quad (10)$$

Figure 4 demonstrates  $\Lambda(T_e)$  calculated for Be ions. The comparison with other available data (the ADAS database) shows a rather good agreement.

We also performed calculations of effective ionization and recombination rates and studied their dependence on plasma parameters. The obtained coefficients will be implemented in the 3D Monte-Carlo neutral transport code EIRENE [17]. The rates were derived from total rate matrix, under quasi-steady-state assumption:  $dN_i/dt = 0$  for all excited states  $e$  except for ground and metastable levels. An example for Be I is shown in figure 5. The essential contribution of the excited states to the effective rates is clearly seen: the effective ionization rate increases monotonically and becomes saturated at high  $N_e$ . The recombination rate behaves nonmonotonically due to competition between the recombination to and the collisional ionization from excited states.

## 4 Conclusion

In this work, a comparison between two independent methods (K-matrix/Coulomb-Born-Exchange and the sophisticated Convergent Close-Coupling) is made for Be I and demonstrates reasonable agreement. Although the CCC method generally provides an excellent accuracy, the use of K-matrix/CBE greatly reduces the computational efforts. Similar K-matrix/CBE calculations (possibly including transitions between fine structure components) can easily be done for other light (or more precisely, small-electron) elements (e.g., for alkali or alkaline earth atoms and their isoelectronic ions).

The collisional-radiative model constructed for Be ions includes new improved set of CCC excitation and ionization cross sections. The steady-state ionization balance, electron cooling rates and radiative power losses were calculated as functions of electron temperature by the NOMAD code. The influence of the excited states on effective ionization and recombination rate coefficients is demonstrated.

## Acknowledgements

This work was supported in part (D. K.) by an EFDA fusion researcher fellowship.



## References

- [1] H. Bolt et al. In: *J. Nucl. Mater.* 307-311 (2002), pp. 43–52.
- [2] H. P. Summers. In: *The ADAS User Manual (version 2.6)* (2004). <http://www.adas.ac.uk/>.
- [3] D. V. Fursa and I. Bray. In: *J. Phys. B: At. Mol. Opt. Phys.* 30 (1997), pp. 5895–5913.
- [4] C. P. Ballance et al. In: *Phys. Rev. A* 68 (2003), p. 062705.
- [5] M. J. Seaton. In: *Proc. Phys. Soc.* 77 (1961), p. 174.
- [6] V. P. Shevelko and L. A. Vainshtein. *Atomic Physics for Hot Plasmas*. IOP, Bristol, 1993.
- [7] D. A. Kondratyev and L. A. Vainshtein. [http://www-amdis.iaea.org/Atom\\_AKM/](http://www-amdis.iaea.org/Atom_AKM/). 2012.
- [8] I. I. Sobelman, L. A. Vainshtein, and E. A. Yukov. *Excitation of Atoms and Broadening of Spectral Lines*. Springer-Verlag, New York, 1995.
- [9] R. D. Cowan. *The Theory of Atomic Structure and Spectra*. University of California Press, Berkeley, 1981.
- [10] Yu. Ralchenko et al. In: *NIST Atomic Spectra Database (version 4.1)* (2011). <http://physics.nist.gov/asd/>.
- [11] S. D. Loch et al. In: *Atomic Data and Nuclear Data Tables* 94 (2008), pp. 257–321.
- [12] I. Bray and Y. Ralchenko. <http://atom.curtin.edu.au/CCC-WWW/index.html>. 1997.
- [13] G. Tachiev and C. Froese Fischer. In: *J. Phys. B: At. Mol. Opt. Phys.* 32 (1999), p. 5805.
- [14] A. Starobinets et al. In: *Physica Scripta* 67 (2003), pp. 500–504.
- [15] P. Mazzotta et al. In: *Astron. Astrophys. Suppl. Ser.* 133 (1998), p. 403.
- [16] Yu. V. Ralchenko and Y. Maron. In: *J. Quant. Spectrosc. Radiat. Transfer* 71 (2001), p. 609.
- [17] D. Reiter, M. Baelmans, and P. Börner. In: *Fusion Sci. Technol.* 47 (2005), p. 172.

## Figure captions

**Figure 1:** Collision strength  $\Omega z^2$  as a function of incident electron energy. “K5” and “K” - K-matrix method with levels up to  $n = 5$  with and without configuration interaction, “B” - Born approximation with account of exchange, “ccc” - convergent close-coupling method (293 states), “ccc0” - convergent close-coupling method [3] (106 states).

**Figure 2:** Electron impact ionization cross section for Be ground state: Born (B), Born with normalization (BN), Born with exchange and normalization (BEN) and CCC calculations.

**Figure 3:** Radiative power loss per unit volume due to line emission, recombination radiation and bremsstrahlung as a function of electron temperature. The total power loss coefficient is shown in red. Dashed lines represent relative concentrations of Be ions.

**Figure 4:** Electron cooling rate for different ionisation stages of Be as a function of electron temperature.

**Figure 5:** Effective ionization and recombination rates as a function of electron temperature for the ground ( $2s^2\ ^1S$ ) and metastable ( $2s2p\ ^3P$ ) states of Be I.

## Figures

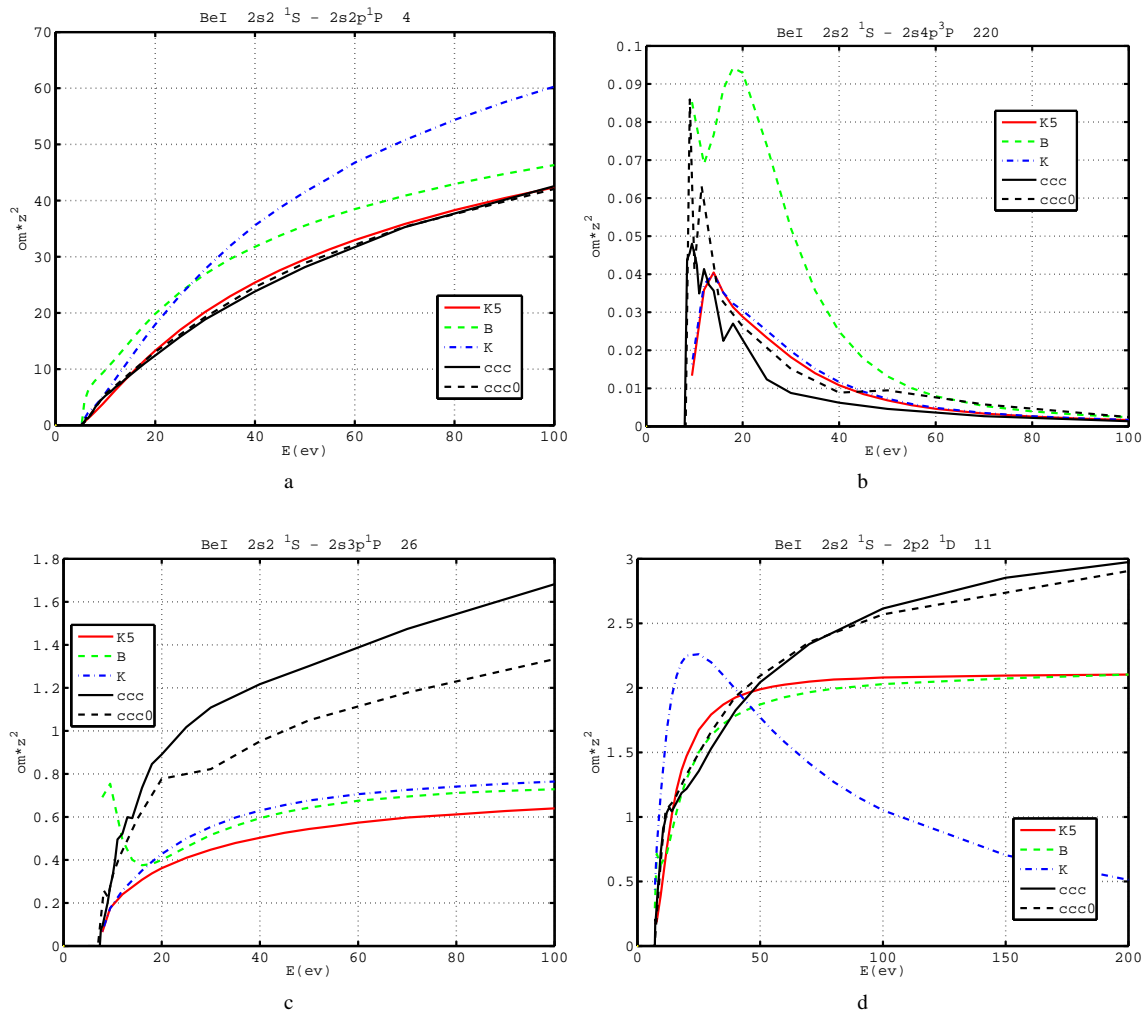


Figure 1: Collision strength  $\Omega z^2$  as a function of incident electron energy. “K5” and “K” - K-matrix method with levels up to  $n = 5$  with and without configuration interaction, “B” - Born approximation with account of exchange, “ccc” - convergent close-coupling method (293 states), “ccc0” - convergent close-coupling method [3] (106 states).

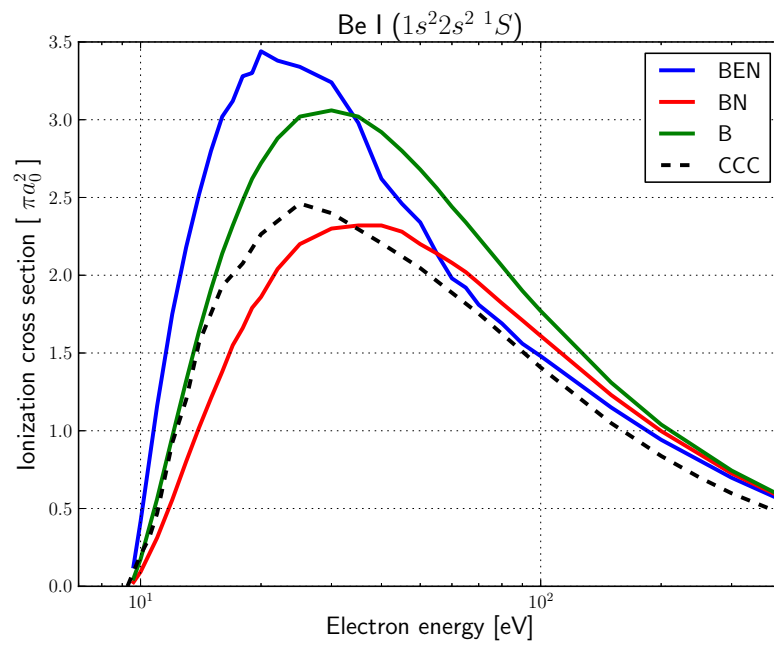


Figure 2: Electron impact ionization cross section for Be ground state: Born (B), Born with normalization (BN), Born with exchange and normalization (BEN) and CCC calculations.

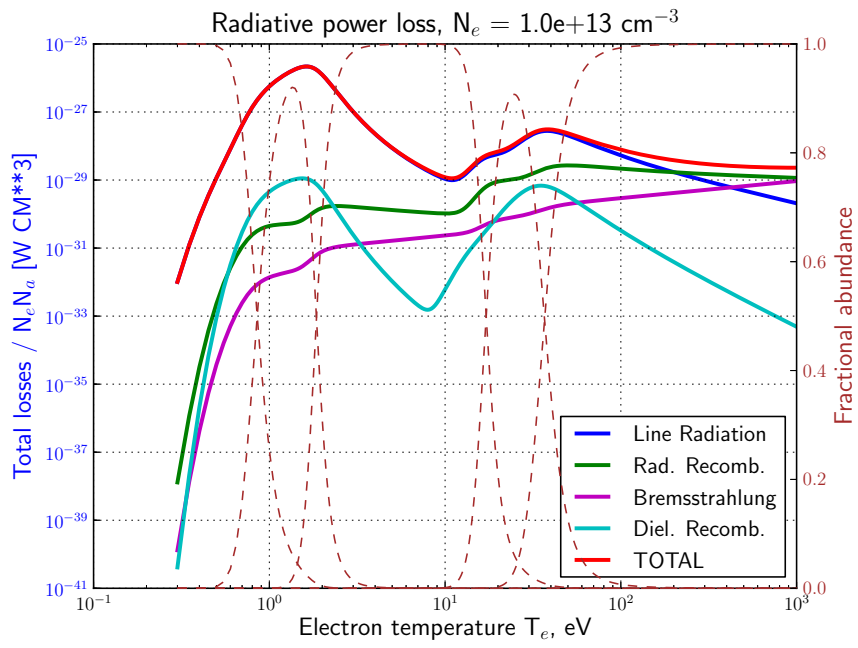


Figure 3: Radiative power loss per unit volume due to line emission, recombination radiation and bremsstrahlung as a function of electron temperature. The total power loss coefficient is shown in red. Dashed lines represent relative concentrations of Be ions.

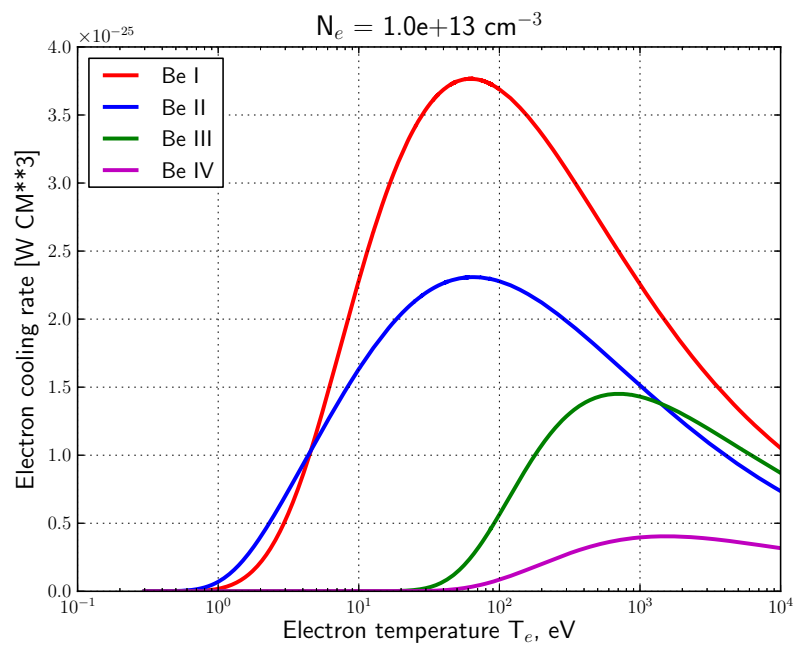


Figure 4: Electron cooling rate for different ionisation stages of Be as a function of electron temperature.

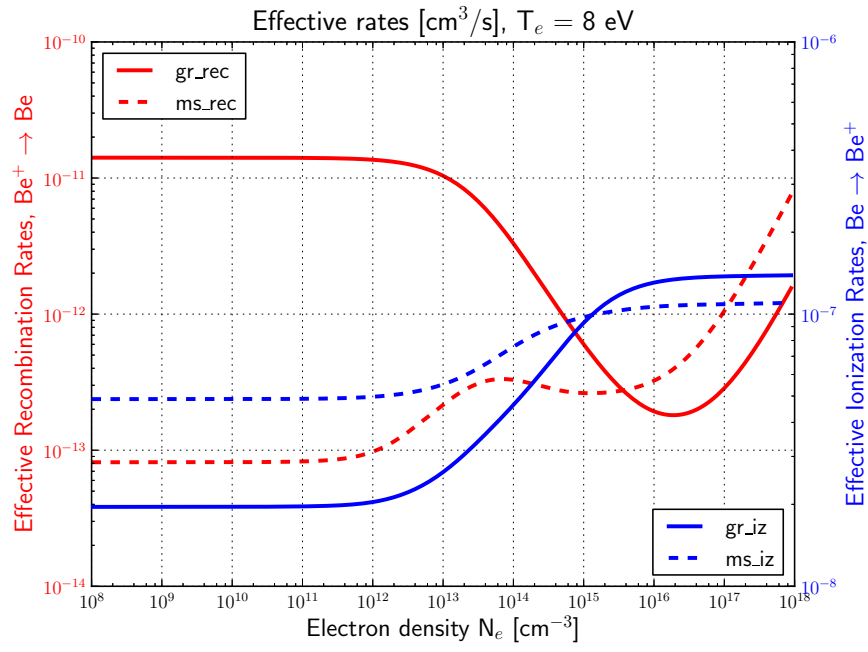


Figure 5: Effective ionization and recombination rates as a function of electron temperature for the ground ( $2s^2\ ^1S$ ) and metastable ( $2s2p\ ^3P$ ) states of Be I.